

FACILITY FORM 802

N66 23787	
(ACCESSION NUMBER)	(THRU)
1	
(PAGES)	(CODE)
04-541014	05
(NASA CR OR TMX OR AD NUMBER)	(CATEGORY)

BALL BROTHERS

RESEARCH CORPORATION

LABORATORIES IN BOULDER, COLORADO AND MUNCIE, INDIANA



GPO PRICE \$ _____
CFSTI PRICE(S) \$ _____
Hard copy (HC) \$ 3.00
Microfiche (MF) \$ 1.50



BALL BROTHERS RESEARCH CORPORATION

BOULDER, COLORADO

FINAL REPORT ENGINEERING BREADBOARD MODEL WOLF TRAP MICROBE DETECTION DEVICE

F65-6

September 8, 1965

Unclassified Report
University of Rochester
Contract No. NsG-209AG-1

PREPARED

D. E. Buckendahl

D. E. Buckendahl
Physicist

L. Ried, Jr.

L. Ried, Jr.
Electronics Engineer

E. Lemberg

E. Lemberg
Research Engineer

APPROVED

M. W. Frank

M. W. Frank
Acting Program Manager



FOREWORD

This report is produced for the University of Rochester under agreement NsG-209AG-1, entitled, "Wolf Trap Microbe Detection Device," and constitutes the final report on Task A, the Engineering Breadboard Model.



ABSTRACT

23787

An experimental microorganism detection device, intended eventually for a Mars landing, is described. The breadboard model optically monitors organism growth in an enrichment culture. Collection of an aerosolized dirt inoculum is accomplished by a gas operated suction pickup. Check-out equipment is described which provides automatic control and data readout. Ability of the device to withstand high temperature sterilization is shown. Recommendations for engineering improvements are made.



CONTENTS

Section		Page
	FOREWORD	ii
	ABSTRACT	iii
	ILLUSTRATIONS	v
1	INTRODUCTION	1-1
	1.1 Background	1-1
	1.2 Objectives	1-2
	1.3 Report Plan	1-3
2	DUST INDUCTION SYSTEM	2-1
	2.1 Introduction	2-1
	2.2 Research Phase	2-1
	2.3 Design Phase	2-9
	2.4 Checkout	2-14
3	CULTURE MEDIUM STORAGE	3-1
4	TURBIDITY DETECTOR	4-1
5	pH DETECTOR	5-1
6	INSTRUMENT ELECTRONICS	6-1
	6.1 General Description	6-1
	6.2 Detector Amplifier	6-3
	6.3 Lamp Regulator	6-7
	6.4 Components	6-9
7	CHECKOUT CONSOLE	7-1
8	INSTRUMENT PERFORMANCE	8-1
9	CONCLUSIONS AND RECOMMENDATIONS	9-1
10	REFERENCES	10-1



ILLUSTRATIONS

Figure		Page
2-1	Jet Pump Configuration	2-3
2-2	Jet Pump Test Schematic for Reduced Atmospheric Pressure	2-6
2-3	Test Results for Jet Pump Nozzle No. 5 at 35-millibar Atmospheric Pressure	2-7
2-4	Test Results for Jet Pump Nozzle No. 5 at Various Atmospheric Pressures	2-8
2-5	Wolf Trap Microbe Detection Device - Assembly	2-11
2-6	Dust Induction System - Schematic	2-12
3-1	Cross-Sectional View of Nutrient Medium Storage	3-2
4-1	Turbidity Detector Diagram	4-2
4-2	Turbidity Detector Spectral Sensitivity	4-4
4-3	Turbidity Detector - Exploded View	4-6
6-1	Two Culture Systems - Block Diagram	6-2
6-2	Detector Amplifier - Simplified Schematic	6-4
6-3	Lamp Regulator - Simplified Schematic	6-8
7-1	Checkout Console - Block Diagram	7-2
7-2	Checkout Console Control Panel	7-3
8-1	Sensitivity Test before Sterilization	8-3
8-2	Sensitivity Test After Sterilization	8-4



Section 1 INTRODUCTION

1.1 BACKGROUND

In 1960, Dr. Wolf Vishniac of the University of Rochester published a paper (Ref. 10.1) in which he suggested some possible life cycles for Martian microorganisms. He further suggested that exploration of this form of life on Mars could be carried out by a device which in principle is a culture tube containing a suitable nutrient medium which can be monitored for changes in acidity and turbidity.

A laboratory device was constructed at Rochester which used phototubes as detectors for light scattered by the turbid culture. A standard laboratory pH probe measured culture acidity. A sealed glass tip, broken on impact with the ground, allowed dust and atmospheric particles to be drawn through a sterile medium into a vacuum reservoir. Relays, actuated by amplifiers and preset to known turbidity and acidity levels, signaled culture growth.

Testing indicated that the device was a very sensitive instrument which could be adapted to a spacecraft environment. Engineering development was needed to produce flight hardware that could survive the rigorous sterilization, launch environment, and Mars landing.



1.2 OBJECTIVES

Engineering effort for the breadboard model was directed toward a first generation instrument that was intended primarily to demonstrate performance capability during field tests and the feasibility of incorporating this capability in a spacecraft oriented design. The design objectives were:

- Two culture systems; one system for inoculation, the other for sterility control or parallel verification
- Sterilization at 145°C for 24 hours
- Dust pickup at an assumed Martian atmospheric pressure of 50 millibars (37 mm Hg)
- Positive detection of one-micron-diameter bacteria at a population of 10^6 organisms per milliliter
- Low power consumption
- Medium storage during sterilization
- pH measurement from pH 4 to 9 with an accuracy of ± 0.25 pH units
- Portable and reusable for field testing
- Simple, reliable design



1.3 REPORT PLAN

This report discusses the subsystems of the instrument and the companion equipment used for instrument control and data presentation. Instrument performance during qualification testing is presented. System performance is compared with design objectives and recommendations for engineering improvements are made in the conclusions.

No attempt is made to discuss the instrument application to biological surveys. Engineering effort has been centered about testing with one microorganism as a standard. Instrument performance with various organism-medium combinations is beyond the scope of the effort.



Section 2

DUST INDUCTION SYSTEM

2.1 INTRODUCTION

The basic requirement was for the design and development of a working breadboard induction system capable of collecting samples of dust from surfaces of average roughness and delivering this dust to a cell for optical observations. The entire operation was to function satisfactorily under conditions simulating those considered to exist on the Martian surface.

The primary objective was to verify the feasibility and limitations of the proposed collection concept through analysis and experimentation. The secondary objective was the development of a design that would ultimately be capable of meeting the spacecraft interface requirements and the environments to be encountered during sterilization, launch, flight, landing, and operation on Mars. Since meeting these objectives would require several systematically planned stages, it was decided to adopt an operational atmosphere of 50 millibars and dry sterilization at 145°C for 24 hours as the initial design parameters.

2.2 RESEARCH PHASE

Preliminary analysis of the initially proposed simple venturi system proved this concept to be impractical at atmospheric pressure of 50 millibars, or less. It was concluded that the jet pump principle, utilizing a supersonic nozzle, offered the best possibility for achieving the ultralow-suction pressures required.



The jet pump, shown in Fig. 2-1, consisted of a delicately matched combination of supersonic nozzle and venturi chamber in which the nozzle efflux gas stream sealed off the venturi throat to provide very low pressures in the chamber.

The nozzle characteristics were such that sonic flow was achieved in the throat followed by a gradual expansion producing supersonic gas velocities and correspondingly low pressures at the nozzle exit. Careful design and fabrication of the assembly was required to prevent choking of the venturi throat by shockwaves with a corresponding complete loss of suction.

To determine the size of nozzle required, the mass flow (m) of a gas through a nozzle throat at Mach 1 was calculated from the expression

$$m = A \sqrt{\frac{2\gamma}{\gamma-1} p_o \rho_o \left(\frac{p}{p_o}\right)^{\frac{2}{\gamma}} \left[1 - \left(\frac{p}{p_o}\right)\right]^{\frac{\gamma-1}{\gamma}}}$$

where

- A = nozzle throat cross-sectional area
- p_o, ρ_o = reservoir gas pressure and density (resp.)
- p = pressure at nozzle exit for nozzle without extension
- γ = ratio of the gas specific heats = 1.4 for dry nitrogen

For a nozzle throat diameter $d = 0.006$ in. and

$$\begin{aligned} p_o &= 250 \text{ lb/in}^2 \text{ a} \\ m &= 5.14 \times 10^{-6} \text{ slugs/second} \end{aligned}$$

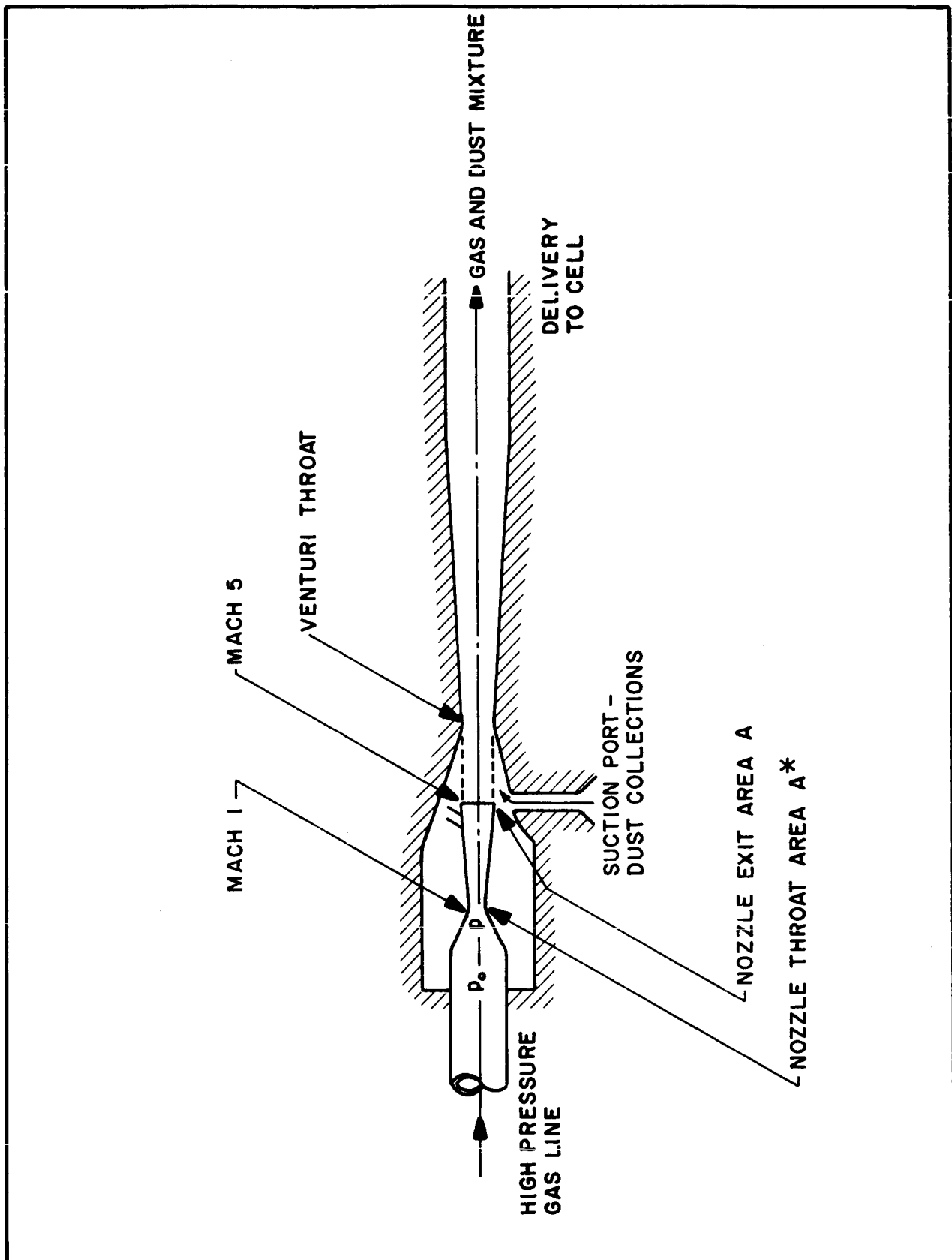


Fig. 2-1 Jet Pump Configuration



From the above expression, it was also deduced that

m is proportional to $d^2 p_o$

or

$$m = K d^2 p_o$$

where K is a constant.

The exit area, A , to obtain the desired exit pressure p^1 was derived from the expression

$$\left(\frac{A}{A^*}\right)^2 = \frac{\frac{\gamma-1}{2} \left(\frac{2}{\gamma+1}\right)^{\frac{\gamma+1}{\gamma-1}}}{\left(\frac{p}{p_o}\right)^{\frac{2}{\gamma}} \left[1 - \left(\frac{p_1}{p_o}\right)^{\frac{\gamma-1}{\gamma}}\right]} \quad (\text{for isentropic flow})$$

where

A^* = throat cross-sectional area

for

$p_o = 159$ psia and $p_1 = 0.3$ psia

$\frac{A}{A^*} = 25$ and the exit mach number = 5

Experimental results showed agreement with the above values within 2 percent.



Developmental testing was carried out in three sections:

- (1) Nozzle tests at earth atmospheric pressure to arrive at the approximate configuration required.
- (2) Tests at various "Martian" atmospheres to confirm the above findings.
- (3) Tests to determine the effects of inducing various quantities of gas.

Figure 2-2 shows the schematic layout of the test setup. The nozzle is shown providing a static suction pressure of 0.27 psia at a Martian atmosphere of 0.5 psia on the right and left manometers, respectively. The test did not utilize air induction into the pick-up entrance port.

Figure 2-3 represents the typical performance behavior (under conditions of no air induction) of nozzle No. 5, which was used in the breadboard. The simulated Martian atmosphere in this instance was 35 millibars.

Figure 2-4 provides a summary of nozzle performance at different atmospheric backpressures. This curve was used to determine the amount of suction to be made available for the breadboard model to simulate Martian conditions.

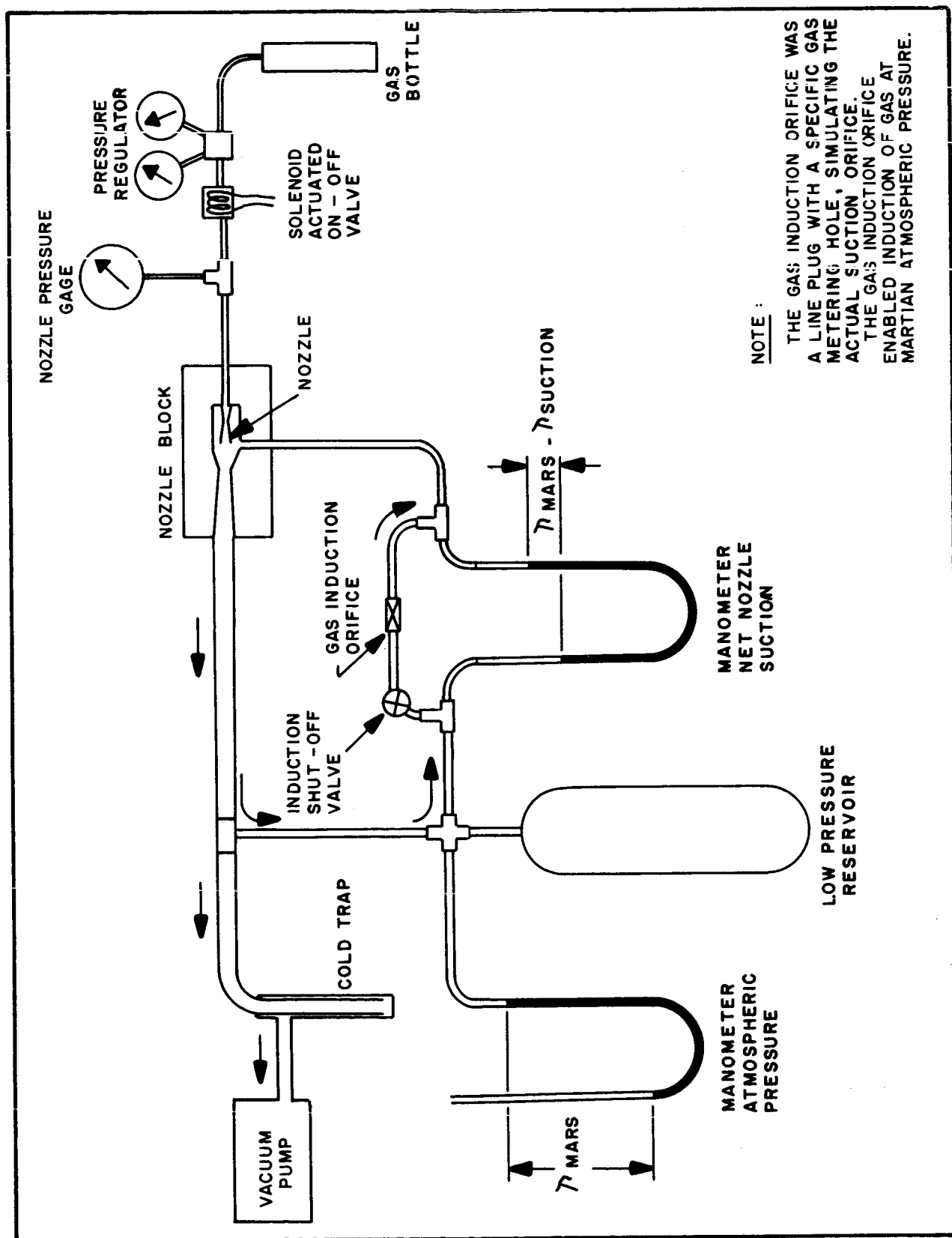


Fig. 2-2 Jet Pump Test Schematic for Reduced Atmospheric Pressure

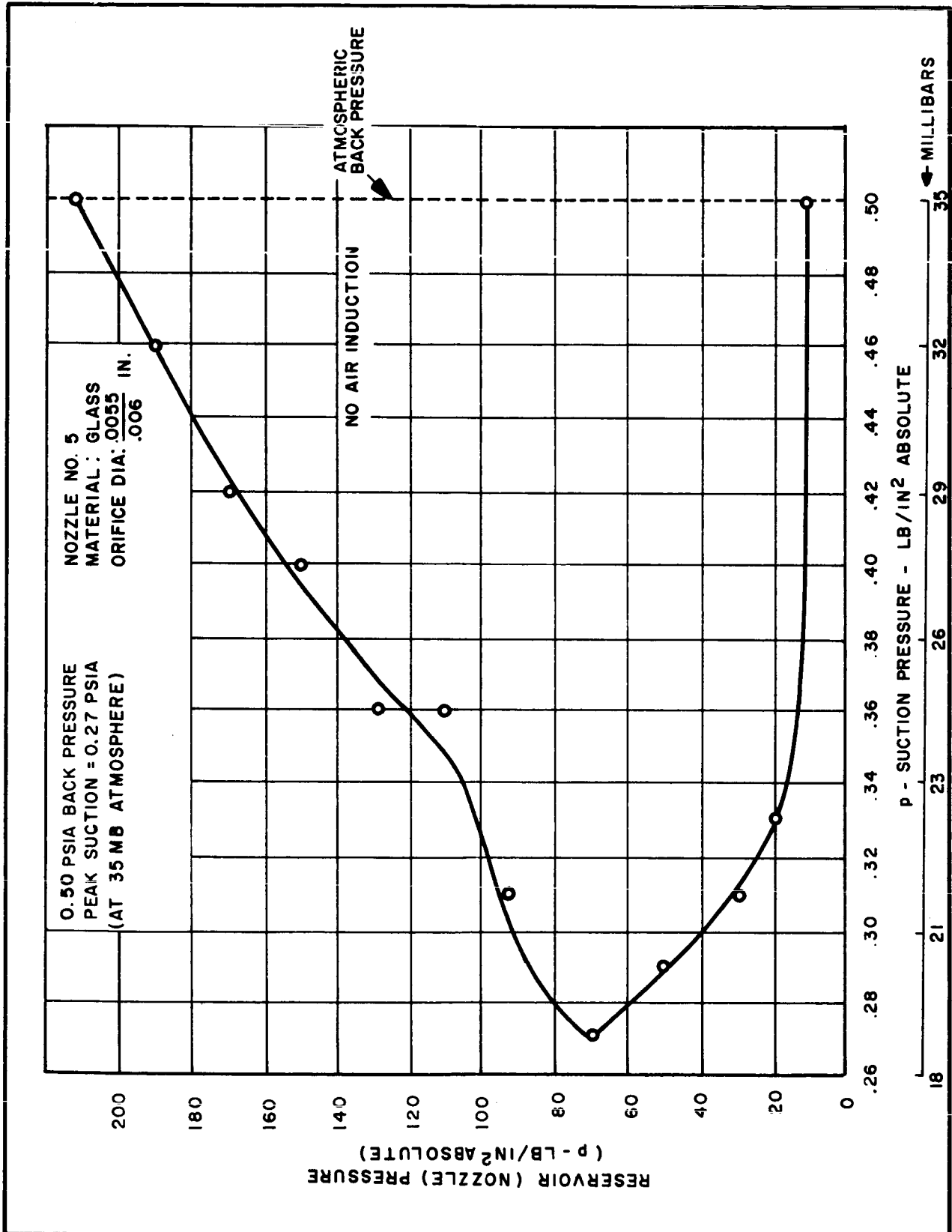


Fig. 2-3 Test Results for Jet Pump Nozzle No. 5 at 35-millibar Atmospheric Pressure

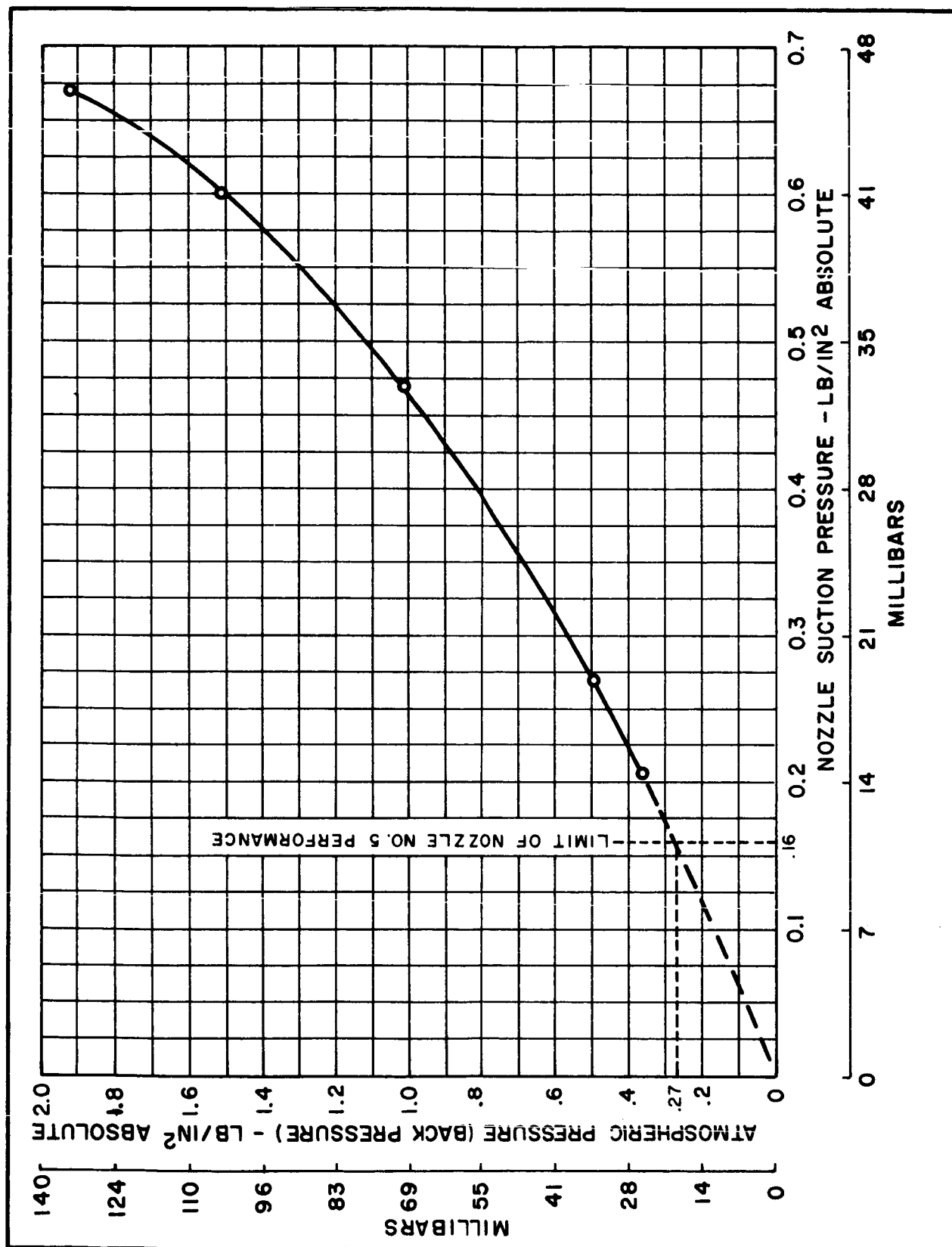


Fig. 2-4 Test Results for Jet Pump Nozzle No. 5 at Various Atmospheric Pressures



The problem of collecting dust was treated in two parts.

(a) Dust Particle Equilibrium in a Vertically Moving Gas Stream

Analysis showed that, in order to keep the maximum size particle (150 microns) suspended in a vertical gas stream for a maximum specific gravity of 3, the stream velocity on Mars must exceed 46 ft/sec. It was therefore felt that gas velocities of 100 to 200 ft/sec should provide adequate energy to ensure elevation and transport of available dust.

(b) Induction Comparison Between Earth and Mars

Dimensional analysis of the significant parameters involved in dust particle suspension showed that for a degree of dust collection on earth equivalent to that on Mars with a 50 mb atmosphere, the earth suction differential must be 3.72 times that attainable on Mars. Utilizing this factor and data from Fig. 2-4, a breadboard design differential of 9 cm mercury was established.

2.3 DESIGN PHASE

The design parameters summarized below were established as a result of the original requirements as well as data derived from the research phase.



- The nozzle was to function in an earth environment, utilizing only the pressure differential equivalent to that available in a 50-millibar Martian atmosphere. The equivalent differential was calculated to be 9 cm mercury. The corresponding nozzle gas pressure was 160 to 200 psi gauge.
- Design operating time: 3 minutes or less, provided sufficient dust was collected.
- Operating voltage: 20 volts dc
- Thermal soak: 24 hours at 145°C (293°F)
- Operating gas: Dry nitrogen
- Soil particle size: 150 microns (0.006 in.) max. soil specific gravity from 1 to 3.
- Martian "g" = $0.38 \times \text{earth "g"}$

Figure 2-5 shows the finished assembly. The cover and trap door were removed for clarity. The pneumatic circuit schematic (Fig. 2-6) provides the circuit outline for the model and the checkout console.

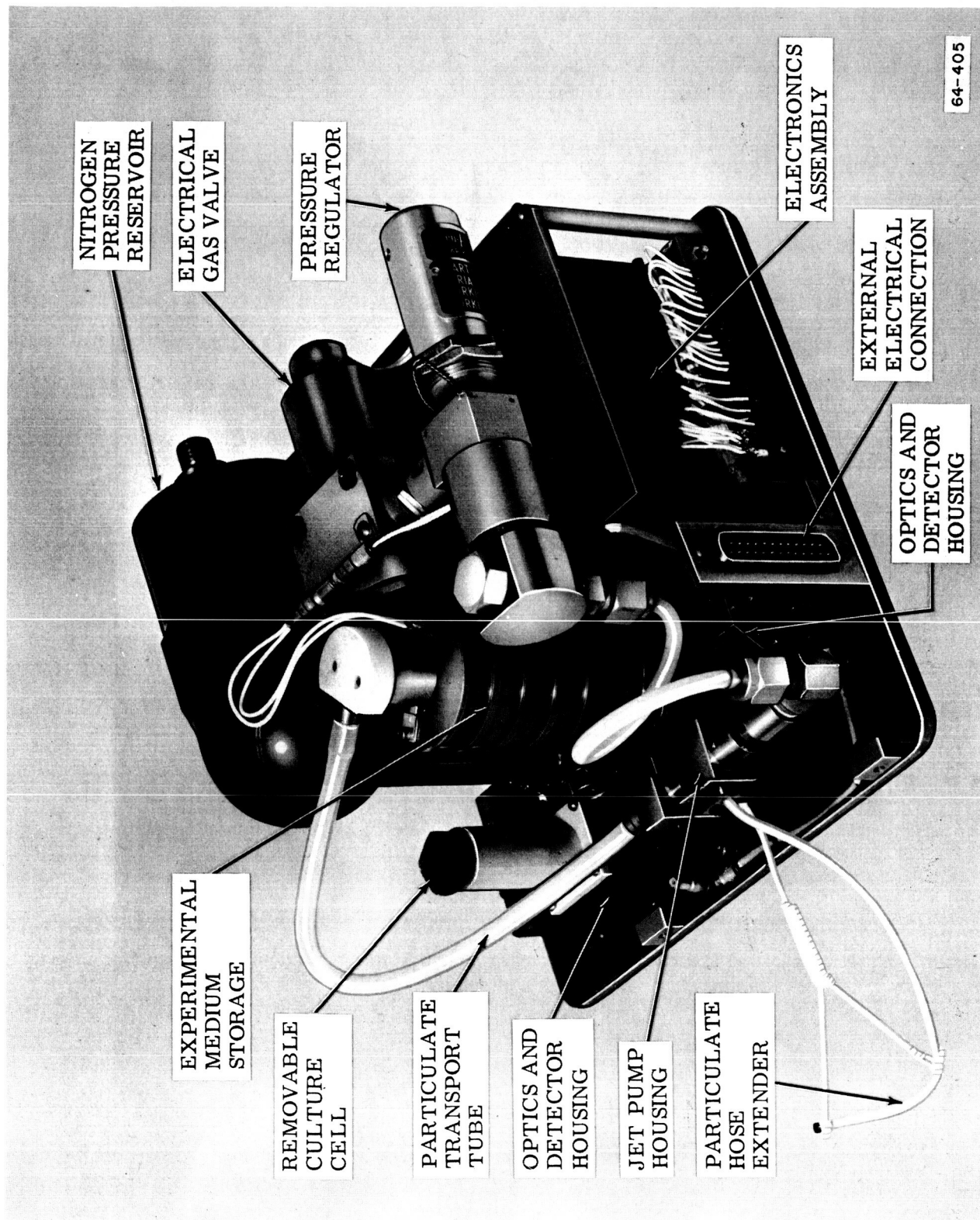


Fig. 2-5 Wolf Trap Microbe Detection Device - Assembly



F65-6

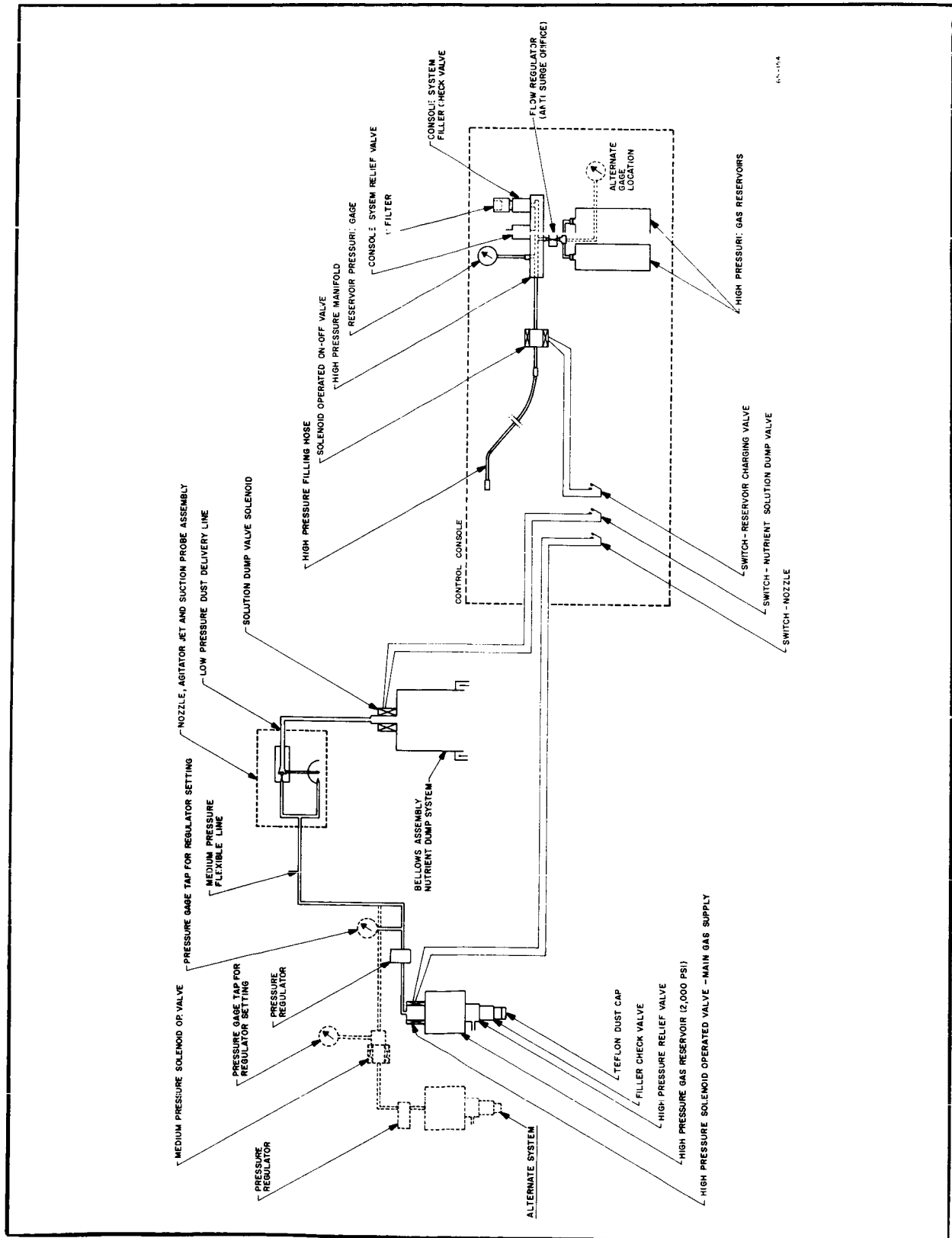


Fig. 2-6 Dust Induction System - Schematic



Gas storage is provided in the high-pressure reservoir, designed to operate at 2,000 psi and tested to 5,300 psi pressure. Fitted into the vessel lid were a filler check valve and a relief valve to prevent accidental overpressurization. From the reservoir, the gas passed through an electrically actuated solenoid on-off valve. The valve originally designed for the OSO spacecraft had all seals replaced with Viton-A "O" rings, was baked at 300°F, and water immersion leak tested at 1,500 psi.

At the pressure regulator gas pressure was reduced to about 200 psi (dependent on adjustment). From there, the gas was transported via the pressure tested (800 psi burst) teflon hose to the nozzle, emerging in the nozzle block at considerably reduced pressure.

The induction suction preset to the specified amount was regulated by axial positioning of the nozzle in the block. The nozzle mount position was secured by two set screws, one of which is shown in Fig. 2-5. The suction caused dust particles to be drawn into the teflon suction hose which was automatically ejected upon release of the lid trap door.

Inducted particles were drawn into and mixed with the main jet stream in the suction chamber and transported via the teflon tailpipe to the cell unit where the dust was deposited due to deceleration of the gas. The carrier gas was vented to the atmosphere.



2.4 CHECKOUT

The pneumatic portion of the console provided a conveniently controlled gas charging device for the breadboard model. The schematic (Fig. 2-6) shows a filler check valve through which the two interconnected gas reservoirs were charged from a dry nitrogen gas bottle. A simple anti-surge orifice, consisting of a 0.015-inch-diameter hole in a 1/8-inch-thick plate, was inserted in the line. The storage bottles were limited to an operating pressure of 1,000 psi, and a relief valve, 1,300 psi, prevented accidental overpressurization. Breadboard gas recharging was facilitated by an electrically operated solenoid valve.



Section 3

CULTURE MEDIUM STORAGE

The medium storage assembly was a device which contained the liquid nutrient medium in a sealed chamber until remote electrical actuation drained the medium into the culture cell. The breadboard design was directed primarily to a device suited for repeated field tests rather than to the final flight configuration.

Figure 3-1 is a cross-sectional view of the storage assembly. The central dust tube carried the aerosolized dust into the lower chamber where the carrier gas velocity was decreased because of the increased cross-sectional area of the chamber. Particulates settled into the culture cell out of the sloped bottom of the chamber while the slowly moving gas escaped through exhaust holes at the top of the chamber. A lip on the outer cover prevented external airborne organisms from migrating into the sterilized system.

After the gas flow stopped, the electrical solenoid was energized, the iron sleeve was attracted upward and impacted the outer cover. The impulse raised the outer cover off the ball retainers and the spring pushed the plunger below the plunger sleeve. This allowed the liquid to be drained into the lower chamber and washed the inducted dust into the culture cell.

The plunger and sleeve were made of teflon to withstand corrosion during sterilization and to minimize medium absorption. Ease of cleaning teflon prevents carryover of medium residue into succeeding cultures using a different medium. "O" rings provided pressure sealing during sterilization.

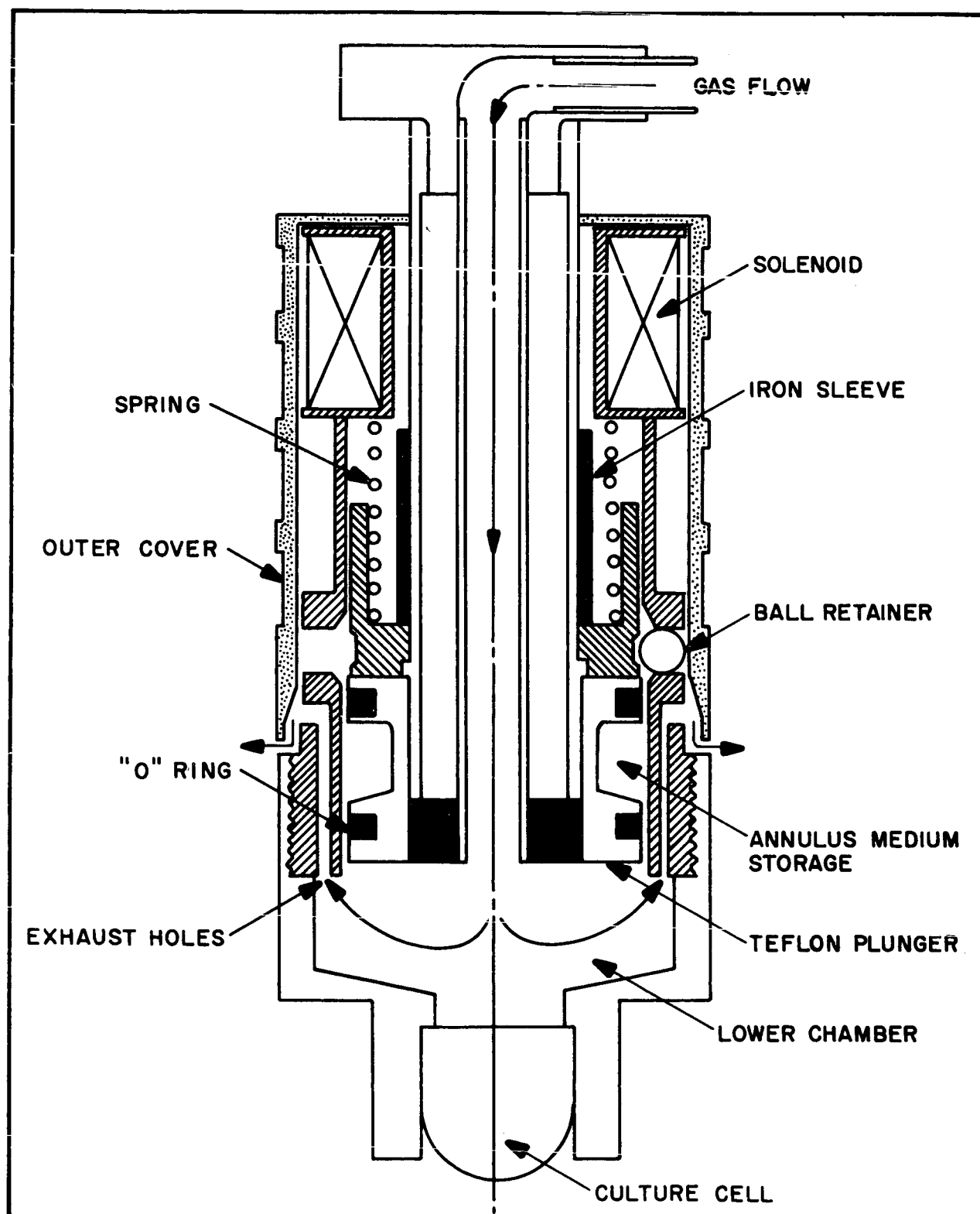


Fig. 3-1 Cross-Sectional View of Nutrient Medium Storage



Section 4

TURBIDITY DETECTOR

The turbidity detector used an in-line optics train which directed intensity regulated, collimated light through the culture medium. An occulting disc allowed only light scattered by dust or organisms in the culture to reach the detector.

In Fig. 4-1, the tungsten lamp was a subminiature device which approximated a point source of light. The corrected collimating lens beamed a narrow pencil of parallel light rays through the transparent culture cell. The imaging lens focused the undeviated light rays into an image of the lamp filament on the occulting dot which blocked direct light transmission to the detector. An organism in the culture scattered (deviated) some of the light rays from their original parallel paths. This scattered light passed around the occulting dot and produced a signal current in the scatter detector cell. Lens aberrations and scratches allowed some light to pass around the occulting dot and caused a fixed background signal. The large imaging lens collected light scattered from the culture and directed it into a highly polished light funnel. The lens-funnel combination assured that light scattered at large angles was collected and reflected onto the detector. The converging funnel also allowed a smaller detector cell area than would be required with a simple lens system. A monitor cell sensed any change in the lamp output and adjusted the lamp current to maintain a constant intensity.

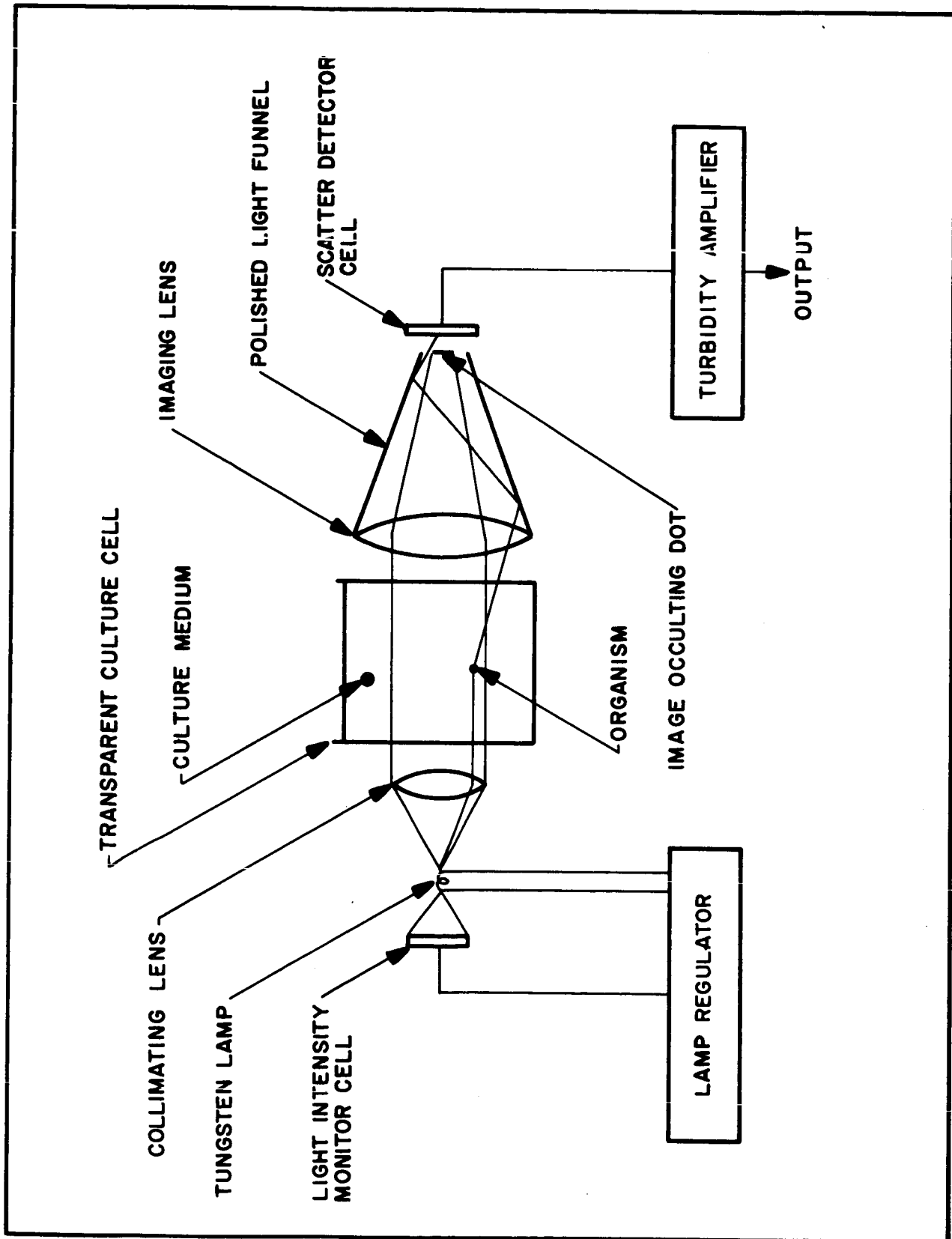


Fig. 4-1 Turbidity Detector Diagram



Both the light intensity monitor cell and the scatter detector cell were diffused junction silicon semiconductors which could withstand high-temperature sterilization. Both cells are made as small as feasible to minimize cell peripheral length which determined electrical leakage, a major cause of system instability. The cells had closely matched spectral response characteristics, important for system temperature stability. Since the output of the cells change as a function of temperature, the lamp current regulator provides thermal stability as well as compensation for lamp variations, power supply shifts, etc. The efficiency of light scattering by small particles is a function of the wavelength of the light, particle size, and scatter angle. Scattering of light having a wavelength approximately equal to the particle size is optimum at small angles (Ref. 10.2). Detector sensitivity is a function of wavelength and angle of incidence. Figure 4-2 shows the relative spectral emission characteristics of the lamp, the spectral sensitivity of the silicon cell, and the combined system sensitivity. The detector was most sensitive to culture particles of 0.9-micron size, but because of the ability of the lens and polished funnel to collect light scattered at large angles, the system would detect particles having a wide size range.

By increasing the breadboard lamp voltage to 1.1 times rated value, lamp light output was increased to 1.4 times rated light output and the scatter signal was increased to 20 times that at the rated lamp voltage. This substantial signal increase was caused by a shift of the emitted light wavelengths into the sensitive region of the silicon cell. Life expectancy of the lamp was reduced from a rated 1000-hour life to 340 hours by this change. It is expected that a lamp having an optimized spectral output for this application may be found.

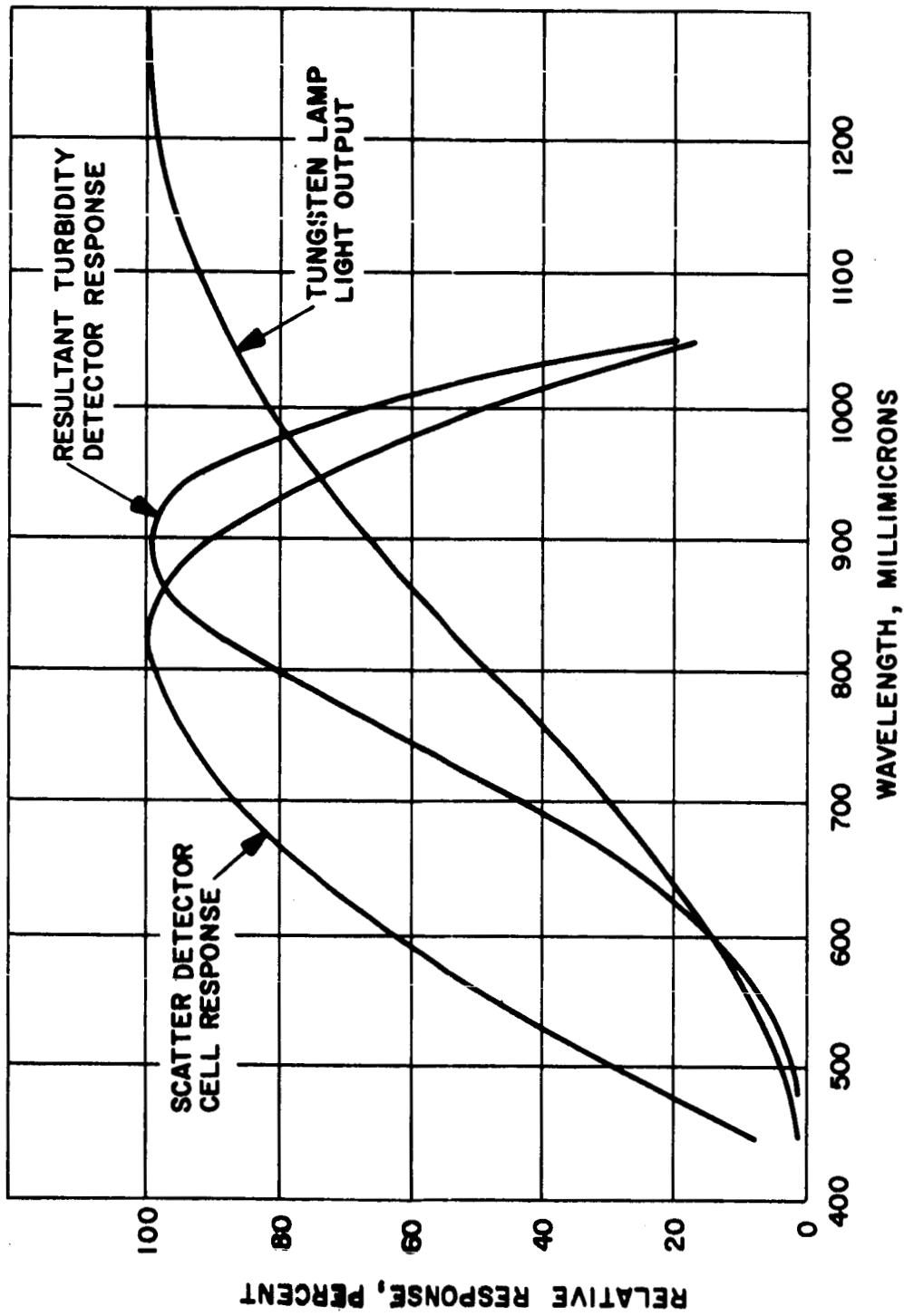


Fig. 4-2 Turbidity Detector Spectral Sensitivity



Figure 4-3 shows the actual detector components excluding the transparent culture cell. Focusing of the filament image on the occulting dot was accomplished by positioning the lamp assembly with the machine screws on the left side of the assembly. The occulting dot, supported on a glass plate, is seen as a black dot in the center of its support ring. The culture cell fits into the central well in the main housing.



F65-6

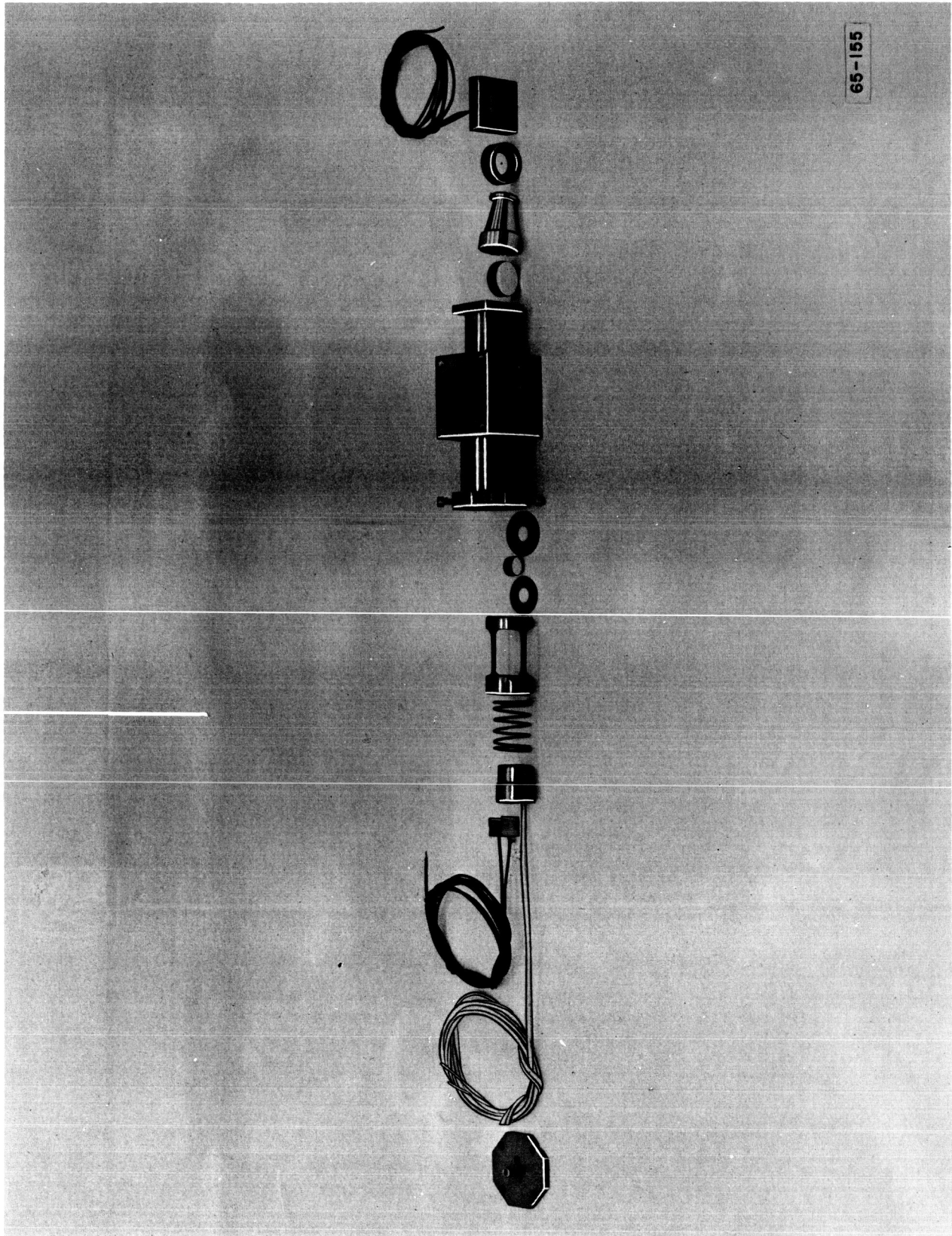


Fig. 4-3 Turbidity Detector - Exploded View



Section 5

pH DETECTOR

The pH detector system was not yet completed since available commercial type pH probes can not withstand high temperature sterilization. A major probe manufacturer indicated that miniature, mechanically rugged probes were feasible, but that guaranteed performance after being heated to 145°C would require a research program. Additional investigation of pH detectors will be required as a major part of the development of an operational system.

A simple dc amplifier circuit for the probes was constructed. Preliminary testing showed a circuit input impedance of 10^{11} ohms, satisfactory for use with the high resistance probes. Thermal drift and long-term stability tests have been delayed until suitable probes became available.



Section 6

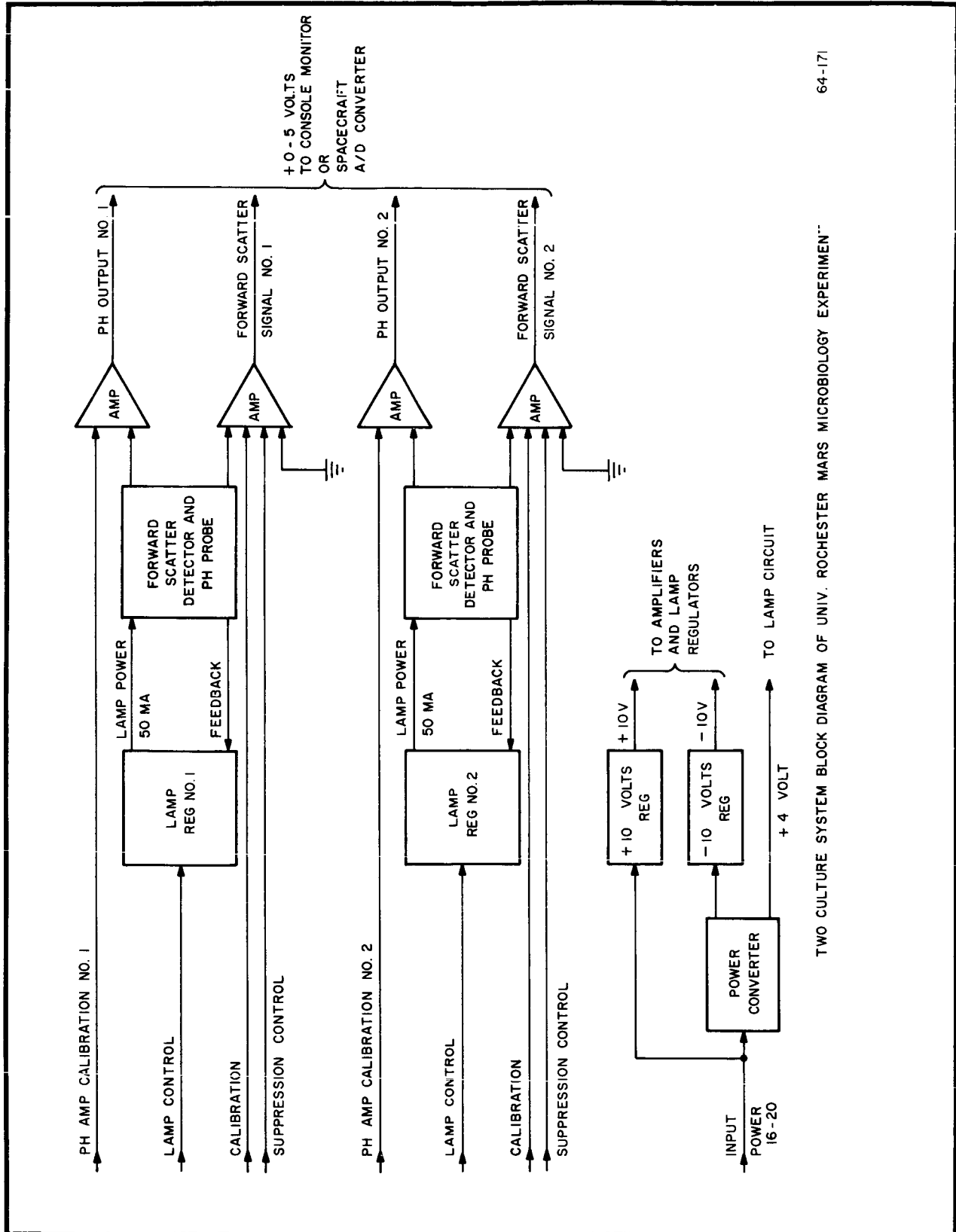
INSTRUMENT ELECTRONICS

6.1 GENERAL DESCRIPTION

A block diagram of the two culture systems is shown in Fig. 6-1. Both detection systems were identical. A lamp regulator used a silicon solar cell in the feedback loop and provided constant lamp illumination. Average power consumption was reduced by energizing the lamp only during 10-second readout intervals. Bulb life was extended by using a current limiter in the lamp supply line to suppress turn-on current surges.

Low-level forward scatter light was detected by a second silicon cell having matched thermal and spectral characteristics with the lamp regulator diode. A narrow-passband, low-level dc amplifier converted the signal current to a voltage output suitable for a zero-to-five-volt spacecraft analog telemetry input. A feedback current amplifier was used instead of a chopper stabilized amplifier since it has considerably fewer components and sufficient stability for the system requirements.

A power converter was used to provide the necessary system voltages from the single battery in the checkout console. The converter will not be used in subsequent models so that little consideration was given to the selection of high temperature components for this circuit. The lamp supply was unregulated and provides approximately four volts at the input of the current limiter. Both dc voltage regulators were three transistor circuits which maintained ± 10 -millivolt output regulation over a 0-degree to 50-degree temperature range.



TWO CULTURE SYSTEM BLOCK DIAGRAM OF UNIV. ROCHESTER MARS MICROBIOLOGY EXPERIMENT

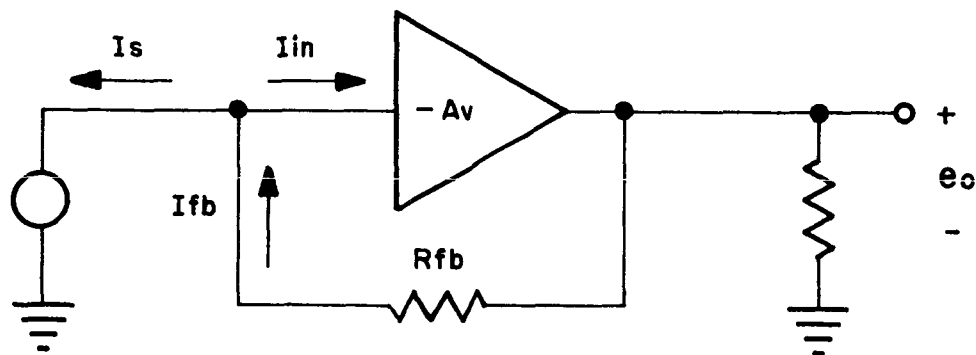
64-171

Fig. 6-1 Two Culture Systems - Block Diagram



6.2 DETECTOR AMPLIFIER

A simplified schematic of the detector amplifier is shown in Fig. 6-2. Actual grounding connections are not indicated in the schematic. The circuit was a high gain, differential input, single ended output amplifier with overall negative feedback. The differential input consisted of ground referenced transistors Q_1 and Q_2 . Transistors Q_1 and Q_2 were on a single header and had matched base-to-emitter voltage temperature coefficients of better than 10 microvolts /°C. The current gain at a 10-microampere collector current was better than 50 at 0°C. Q_1 was biased at one microampere collector current. Noise and collector-base leakage were minimized by biasing the collector voltage of Q_1 at a low voltage. High beta transistors were used to achieve a large open-loop gain. The importance of high open-loop gain and low base current to Q_1 is shown by considering the equivalent circuit and generalized analysis as follows:



The solar cell, shown as a current path, is assumed to have negligible internal leakage. This is valid if the amplifier input impedance is very low, on the order of a few ohms.

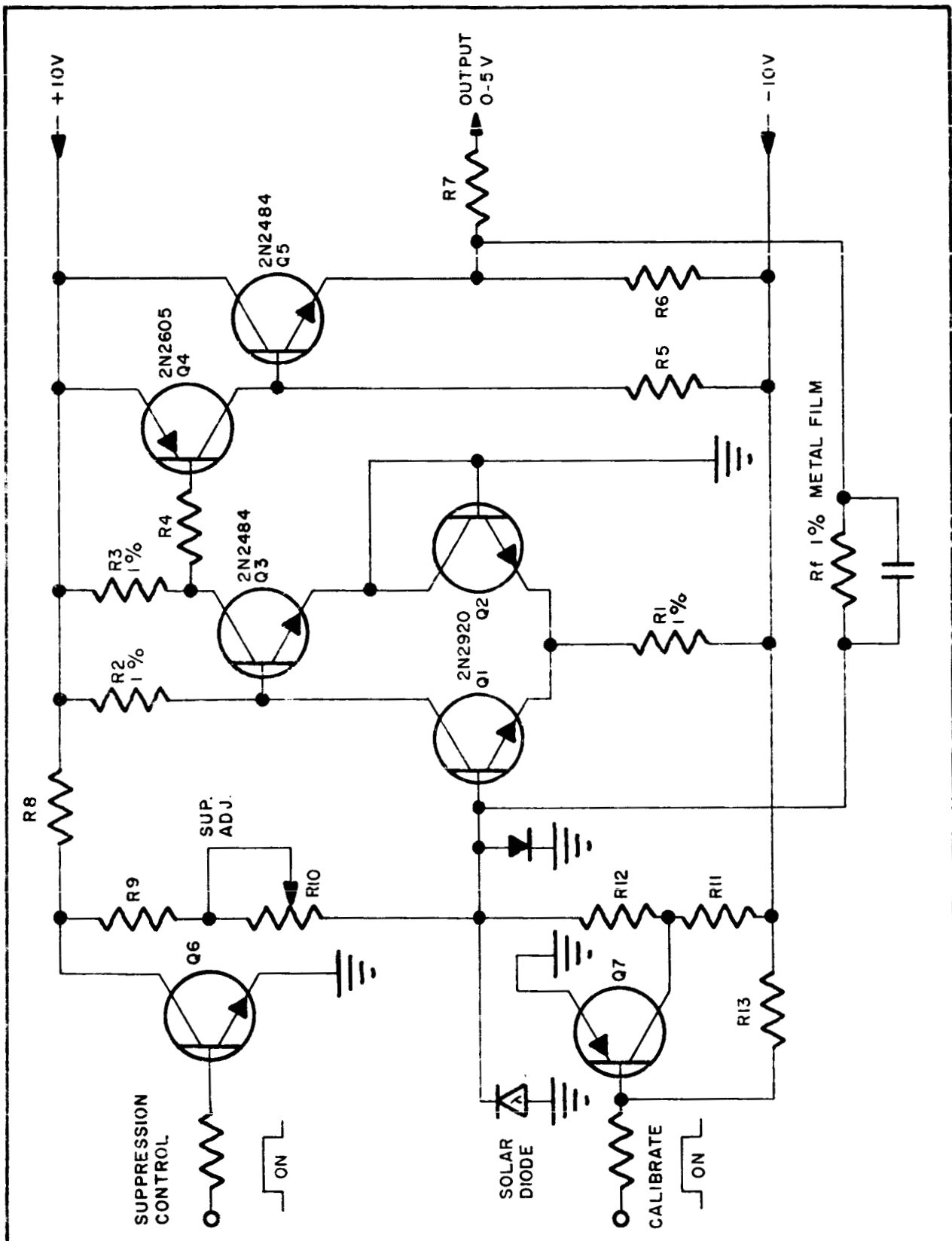


Fig. 6-2 Detector Amplifier - Simplified Schematic



The output voltage is given by:

$$e_o = f(I_s) \quad (6.1)$$

$$e_o = -A_v I_{in} \quad (6.2)$$

and at the input node:

$$I_{in} = -I_s + I_{fb} \quad (6.3)$$

combining equations (6.2) and (6.3) we have:

$$e_o = -A_v (-I_s + I_{fb}) \quad (6.4)$$

Since the summing node at the input is very close to ground or zero volts, the feedback current is:

$$I_{fb} = \frac{e_o}{R_{fb}} \quad (6.5)$$

Equation (6.4) now becomes:

$$e_o = -A_v \left(-I_s + \frac{e_o}{R_{fb}} \right) \quad (6.6)$$

Solving for the output voltage:

$$e_o = I_s \left(\frac{A_v}{1 - A_v/R_{fb}} \right) \quad (6.7)$$



Since $A_v \gg 1$ the limiting value for e_o will be:

$$e_o = -I_s R_{fb}$$

The gain is therefore dependent on only the feedback resistor R_{fb} .

A similar analysis would show that the input impedance is close to:

$$\frac{R_{fb}}{A_v + 1}$$

For an input current range of 1500 nanoamperes and $R_{fb} = 3.2$ meg ohms, the amplifier performance values listed below were experimentally determined. All currents are referred to the input.

Gain	= 3.2 volts/microamp
Long-term drift	= ± 0.5 nanoampere over 3 days at $\pm 4^\circ\text{C}$
Thermal drift	= ± 1.5 nanoamperes from 0 to $+50^\circ\text{C}$
Output voltage range	= 0 to 5 vdc

The circuit provided 0.1 percent resolution for 1500 nanoampere maximum signal. Instrument stability was greatly dependent upon the leakage current characteristics of the solar cell. With an unilluminated solar cell, the instrument thermal drift increased to about ± 4 nanoamperes over the temperature range of 5°C to 50°C .

Transistors Q_6 and Q_7 were used for background suppression and calibrate controls. A positive current, opposite to the signal polarity, could be adjusted from 400 to 900 nanoamperes to set the output voltage near zero



with no scatter signal other than background. Suppression was removed when the lamp was turned off to prevent a negative amplifier output voltage with no background light.

6.3 LAMP REGULATOR

The lamp regulator circuit shown in Fig. 6-3 was similar to the detector amplifier circuit except that the feedback current was the solar diode output caused by lamp illumination. The lamp adjust control was set to produce a 50-milliampere lamp current at a diode current of about 200 microamperes. The stability of the regulator could not be directly measured by monitoring the diode current since insertion of a meter in the feedback loop produced erratic regulation of introduced electrical noise in the circuit. The total system stability described below as compared to the detector amplifier stability is a result of spectral mismatch of the regulator and detector diode and the thermal drift of the regulator circuit. Values are output referred to the input.

	<u>Detector Amp</u>	<u>Total System</u>
Long-term drift	$\pm 0.5 \text{ na}$	$\pm 1.0 \text{ na}$
Thermal drift		
0 - 50°C	$\pm 1.5 \text{ na}$	
5° - 25°C		- 20 na
25° - 50°C		+ 10 na

The lamp current increased about 1 percent from the 25°C value when the system temperature was reduced to 0°C and decreased about 1 percent at + 50°C. This change is caused by the change in spectral response of the regulator diode with temperature.

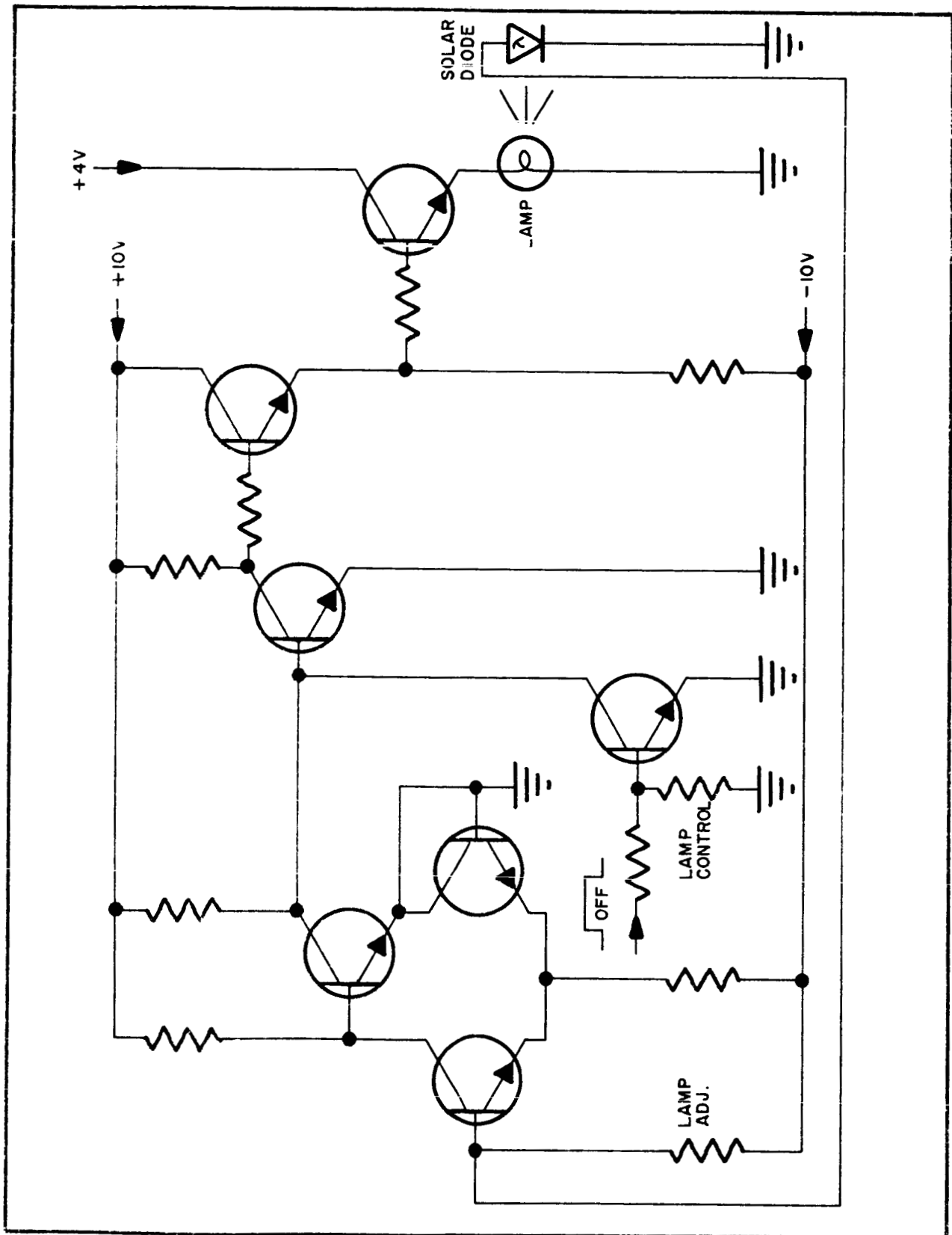


Fig. 6-3 Lamp Regulator - Simplified Schematic



6.4 COMPONENTS

Component selection was based on survival testing and not on prepared parts lists. The capacitors used in the converter were not rated for the sterilization temperature although no failure or value change was detected through final testing. The converter would not be used in subsequent models because positive and negative polarity voltage sources would be assumed available.

Two failures occurred during sterilization testing. After the first hour at 150°C, one metal film resistor developed an intermittent opening. No other component failures occurred during two 3-hour, two 12-hour, and one 24-hour subsequent sterilization tests at 150°C. A cold solder joint opened during the last test. All resistors were either metal film or carbon composition. All active elements were silicon planar passivated devices.



Section 7

CHECKOUT CONSOLE

The block diagram of the checkout console is shown in Fig. 7-1. Figure 7-2 is the control panel of the assembly, mounted in an 18-inch by 25-inch metal suitcase. The primary functions of the console were:

- (1) Supply power to the instrument
- (2) Monitor instrument voltage and current
- (3) Provide readout for instrument signal outputs
- (4) Provide manual control for certain instrument functions
- (5) Provide a programmed timing sequence for automatic control of instrument functions
- (6) Provide transport storage for the instrument and accessory cables

The rectangular hole in the panel (Fig. 7-2) accommodated the instrument which was secured with captive screws. The console controls are described below.

- Power mode - select internal battery power or external line power, charge internal battery
- Shroud eject - actuate solenoid to open experiment door and release dust pickup arm
- Sample induct - open experiment solenoid gas valve to dust pickup pneumatic system

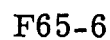


Fig. 7-1 Checkout Console - Block Diagram



Fig. 7-2 Checkout Console Control Panel



- Nutrient dump - actuate solenoid to drain nutrient medium into culture
- Automatic sequencing - initiates sequence for shroud eject, timed sample induct, nutrient dump and timed data readout interval
- Data readout interval - adjusts timing period for parallel data readout
- pH calibrate - injects preset signal into pH amplifier
- Scatter calibrate - injects preset signal into detector amplifier
- Scatter suppress - removes electronic suppression of background scatter light
- Experiments volts adjust - changes console power supply voltage to experiment to check regulation
- Meter selector - monitors voltage and current on common panel meter
- Pressure reservoir - storage of high-pressure nitrogen gas for experiment dust pickup pneumatics



Automatic sequencing was timed from a one-cycle-per-second electronic clock which advanced decade scalers to provide adjustable preset timing for sample induction and data readout. The automatic mode sequence always started with immediate shroud ejection and a programmed sample induction time and was followed by nutrient dump. Parallel data readout occurred for ten seconds at the start of the sequence and at subsequent programmed intervals. Protection from accidental electrical transient actuation of experiment functions was obtained by placing each function switch in the "safe" position. The pushbutton "manual" switches would override the automatic function safety switches.

The "experiment volts adjust" varied the voltage output of a transistor regulating circuit which was powered from either power line rectifier or the internal batteries. For a normal output to the experiment electronics of 18 volts, the current drains were:

- 12 milliamperes - experiment lamps off
- 36 milliamperes - one lamp on
- 44 milliamperes - both lamps on

Internal batteries were two 12-volt, rechargeable nickel-cadmium cells connected in series. The console charging circuit was a constant voltage source limited to a maximum 150-milliampere charging current. Fully charged, the battery would operate the experiment in the automatic mode for 24 hours.



Section 8

INSTRUMENT PERFORMANCE

Dust pickup was accomplished where the particulate hose extender, shown in Fig. 2-5, was forced onto the ground by a spring-loaded Y arm after the trap door was released. Dirt particles under 0.03 inches dimension were drawn into holes on the bottom side of the extended hose, up through the jet pump, and then into the culture cell. Only those particles immediately near the holes could be acquired, typically 1 milligram for average garden soil and several milligrams for sandy soils. Required nozzle pressurization time was about 4 seconds. The pressure reservoir charged to 1000 psi provided 136 seconds of induction time, but valve leakages reduced the time to 34 seconds after 24 hours at 150°C. Loss of pressure was caused by a leaky metal-to-metal seat in a pressure safety valve installed in the reservoir.

The medium storage device was tested twice for 12 hours each at 150°C using distilled water instead of broth to avoid possible O-ring sealing with dried solids. In both tests 10 percent of the total 2.5 cc water was lost. The cause of this was imperfect seating of the O-rings against machining marks in the teflon outer sleeve. The lightweight magnesium outer cover showed some surface corrosion as a result of the heat and steam from the escaping water.

Microorganism detection sensitivity tests were performed using strain K-500 E. Coli cultured in a utility beef broth which had been filtered to have residue particles less than 0.4 microns. The inoculum was several



drops of broth culture grown from a specimen obtained from the local university. Figures 8-1 and 8-2 are plots of the actual data obtained during the tests done, respectively, before and after a total system sterilization for 24 hours at 150°C. Population verification was done by performing a triplicate plate count utilizing a two-layer technique. The terminal plate count was performed when the signal had increased 20 nanoamperes (referred to the input) above background, a purely arbitrary figure which would definitely allow an unequivocal growth conclusion. The graphs show a good fit exponential increase curve which closely corresponds to the data points. Culture system No. 2 has greater sensitivity caused by a better match of the occulting disc size to the filament image. This match just blocks the undeviated light rays from the detector cell but allows rays deviated at very small angles to miss the occulting disc and be detected.

The instrument detector circuit was somewhat unstable at temperatures below 25°C, as discussed in Section 6.3. The cause of this thermal drift was a differential change of output between lamp regulator and turbidity amplifier detector cell. Better matching of the spectral response characteristics of the two cells would have lessened the effective thermal drift.

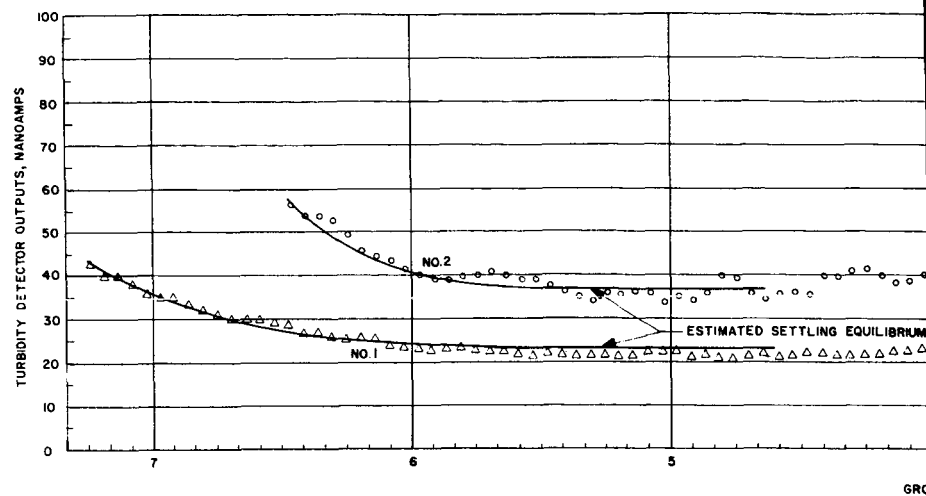
The checkout console performed all functions required by it. Weight of the suitcase housed instrument, including stowed instrument package and cabling, was about 50 pounds. The fully charged internal batteries were able to operate the instrument for 24 consecutive hours.

BEFORE STERILIZATION SENSITIVITY TEST
WOLF TRAP BREADBOARD, SEPT. 17, 1964

CULTURE TEMP: 23°C (NOMINAL)
ORGANISM: E. COLI. K-12, TAKEN FROM OLD SLANT
INOCULATION LEVEL: 10^3 /ml (est)
BROTH: 0.8% BBL & 1% DEXTROSE FILTERED TO $< 0.4\mu$

CHART SCALES: 3 INCHES/HOUR
100 DIVISIONS = 0.320 VOLTS = 100 NANOAMPS
TERMINAL PLATE COUNT: TWO LAYER PLATE IN TRIPLICATE
WEIGHTED AVERAGE VALUE

NO. 1 SYSTEM - 6.45×10^4 /ml
NO. 2 SYSTEM - 3.78×10^4 /ml

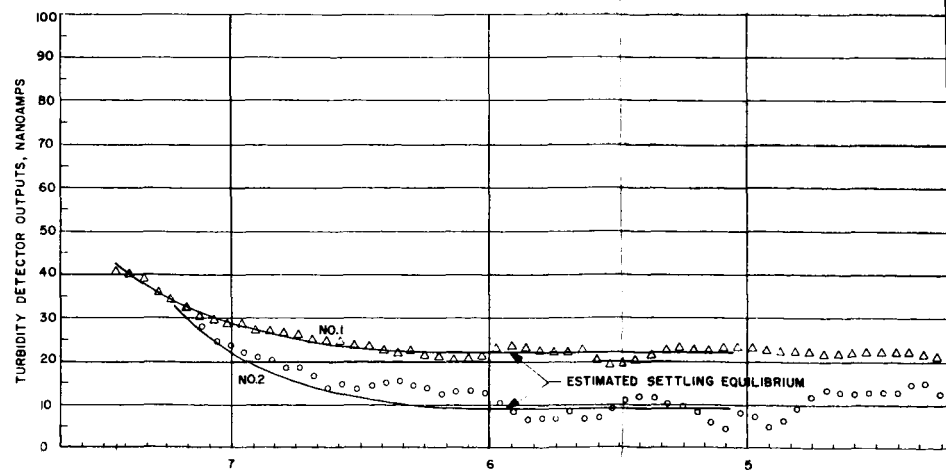


AFTER STERILIZATION SENSITIVITY TEST
WOLF TRAP BREADBOARD, SEPT. 18, 1964

CULTURE TEMP: 23°C (NOMINAL)
ORGANISM: E. COLI. K-12, TAKEN FROM FRESH CULTURE
INOCULATION LEVEL: 7×10^2 /ml (est)
BROTH: 0.8% BBL & 1% DEXTROSE FILTERED TO $< 0.4\mu$

CHART SCALES: 3 INCHES/HOUR
100 DIVISIONS = 0.320 VOLTS = 100 NANOAMPS
TERMINAL PLATE COUNT: TWO LAYER PLATE IN TRIPLICATE
WEIGHTED AVERAGE VALUE

NO. 1 SYSTEM - 5.02×10^4 /ml
NO. 2 SYSTEM - 3.40×10^4 /ml





INPUT
E.

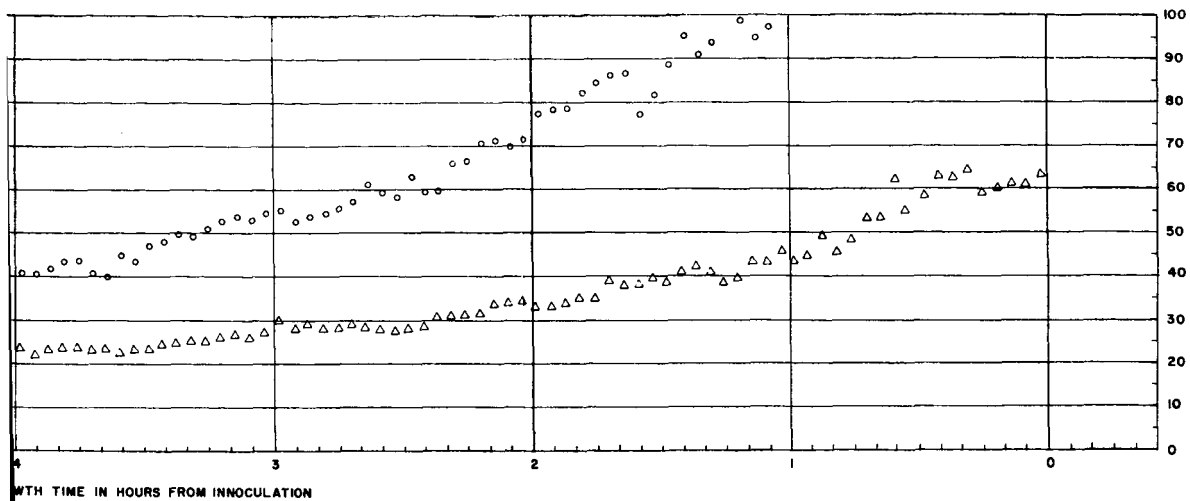


Fig. 8-1 Sensitivity Test Before Sterilization

INPUT
DATE.

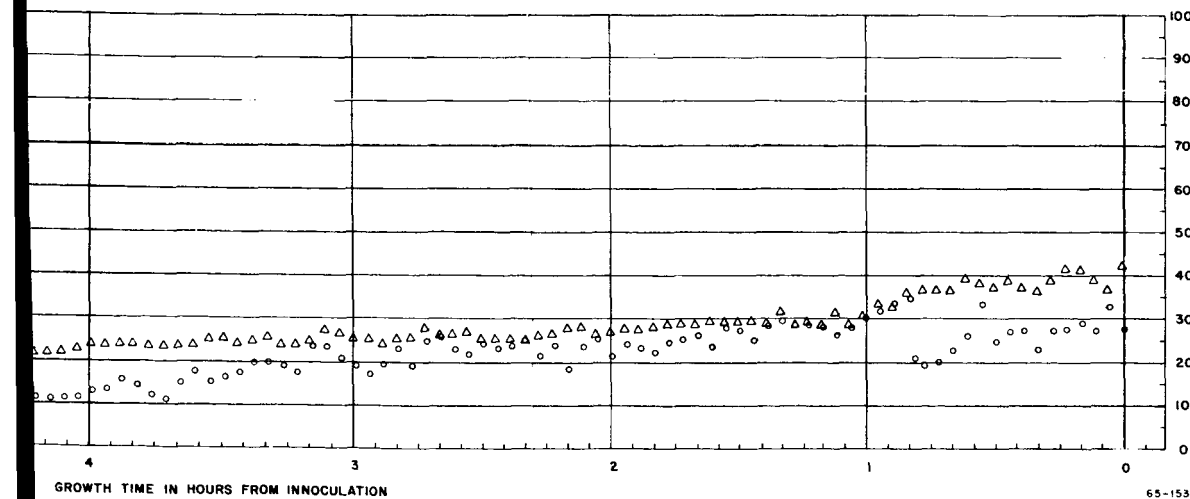


Fig. 8-2 Sensitivity Test After Sterilization



Section 9

CONCLUSIONS AND RECOMMENDATIONS

Total system performance fulfilled the design objectives and provided a useful tool for laboratory and field evaluation of the organism detection concepts. Valve and field leakages, corrosion effects, and some thermal instability require that some care be exercised in the total operation of the system. Successful heat sterilization of the total electronic system demonstrates that the basic design is quite adaptable to an advanced model. Attainment of a detection sensitivity of about 10^4 organisms per milliliter in a breadboard model phase was a decided improvement over commercial nephelometry techniques.

An objective system review produced some specific recommendation for design changes. These are listed below:

SYSTEM PACKAGING

- Separate console electronics, experiment package and gas reservoir system into separate smaller packages for ease of handling.

DUST PICKUP

- Rupture diaphragms should be used in place of valves for positive gas reservoir sealing.



- The method for extending the dust pickup hose should be improved to provide positive contact with any terrain contour.
- Motion of the dust pickup hose during operation would provide for greater dust sample acquisition.

TURBIDITY DETECTOR

- The silicon detector cells should have greater response at the red wavelengths to improve signal and cells should be closely matched in each culture system.
- A more intense, longer life tungsten lamp should be used.
- Good surface quality lenses, free from manufacturing scratches, would reduce scattered light background.

INSTRUMENT ELECTRONICS

- All components should undergo preinstallation bakeout at a temperature above 150°C.



Section 10
REFERENCES

- 10.1 W. Vishniac, "Extraterrestrial Microbiology,"
Aerospace Medicine, Vol. 31, August 1960, pp. 678-680
- 10.2 H. C. van de Hulst, Light Scattering by Small Particles, New
York, J. Wiley Sons, 1957.